Theory of core-level inelastic X-ray scattering spectra and partial local densities of states in low-Z atom crystals

1994 J. Phys.: Condens. Matter 6 11045

(http://iopscience.iop.org/0953-8984/6/50/014)

J. Phys.: Condens. Matter 6 (1994) 11045–11056. Printed in the UK

Theory of core-level inelastic x-ray scattering spectra and partial local densities of states in low-Z atom crystals

R V Vedrinskii, V L Kraizman, A A Novakovich, G Yu Machavariani and V Sh Machavariani

Institute of Physics, Rostov State University, Stachky Avenue 194, Rostov-on-Don 344104, Russia

Received 22 June 1994

Abstract. A method for calculating the double-differential cross sections of the inelastic x-ray scattering (IXS) associated with low-Z-atom K-level excitation of solids is proposed. We have included both the first- and the second-order contributions of one-electron perturbation theory. The second-order contribution is shown to be significant only for comparatively small initial photon energy ($\hbar\omega_0 < 2$ keV). The first-order term is proved to be determined by p partial local densities of electron states (p LDOS) whereas the second-order term is determined by s LDOS. An expression is proposed which enables us to determine the p and s LDOS from experimental IXS spectra measured for different initial photon energies and transferred momenta. Using available experimental IXS spectra and x-ray absorption spectra we have determined the π^* and σ^* p LDOS for graphite crystal. The results obtained are compared with the theoretical π^* and σ^* LDOS calculated using the full multiple-scattering method. The calculated and experimental LDOS are in reasonable agreement, both as regards peak positions and absolute values.

1. Introduction

Information about the local density of unoccupied electron states (LDOS) in solids is of great importance for studies of the chemical bond and local atomic structure in crystals and amorphous media. The widespread experimental technique that provides direct information about the LDOS in solids and molecules is x-ray absorption spectroscopy (XAS). Being convenient for the deep atomic core levels, XAS is faced with significant difficulties in the case of soft-x-ray spectra because of the short mean free path of soft x-rays in solids. Not long ago an alternative technique was proposed [1] which was shown to provide information similar to that provided by XAS but which appeared to be much more convenient for studies of the shallow-core-level spectra. This technique known as inelastic x-ray scattering (IXS) spectroscopy [1, 2] is based on the treatment of the spectra of hard x-rays being inelastically scattered from the crystal which undergoes electron excitation during x-ray scattering. In the case of excitation of a definite core level, the x-ray energy loss is determined by the final energy of the excited electron, and consequently the probability of x-ray inelastic scattering should be connected with the LDOS at the excited atom position.

The calculations of the IXS cross sections are based on the well known Hamiltonian of the electron–photon interaction $\hat{W}_{e\gamma}$ involving two terms:

$$\hat{W}_{e\gamma} = -\frac{e}{mc}\hat{A}\cdot\hat{p} + \frac{e^2}{2mc^2}\hat{A}^2 = \hat{W}_{e\gamma}^{(1)} + \hat{W}_{e\gamma}^{(2)} \tag{1}$$

where $\hat{p}$ is the electron momentum operator and $\hat{A}$ is the vector-potential field operator.

0953-8984/94/5011045+12$19.50

The term $\hat{W}_{e\gamma}^{(2)}$ is small in comparison with $\hat{W}_{e\gamma}^{(1)}$ but it is responsible for the first-order perturbation theory contribution to the IXS amplitudes whereas the largest contribution due to the main term $\hat{W}_{e\gamma}^{(1)}$ is of second order nature. In the case of a homogeneous electron gas the last contribution is exactly equal to zero and therefore the IXS amplitude is determined by the $\hat{W}_{e\gamma}^{(2)}$ term of the Hamiltonian. In [1,2] the theory for inelastic photon scattering from the homogeneous electron gas developed earlier [3] to describe the IXS spectra of solids was employed. There is no doubt that this theory provides an adequate description of the IXS spectra associated with the excitation of the valence band delocalized electrons. Meanwhile the second-order contributions to the IXS cross section resulting from the $\hat{W}_{e\gamma}^{(1)}$ term do not vanish in the case of the spectra associated with the excitation of the core-level localized electrons. Consequently the core-level IXS spectra should be treated more thoroughly.

In section 2 of the present paper the general one-electron theory for the core-level contributions to the IXS spectra is developed, which enables us to include both the first- and the second-order terms. In section 2 a method is also proposed which enables us to determine the partial LDOS from the experimental IXS spectra and x-ray absorption spectra which are formed owing to the K-level near-edge excitation of low-Z atoms. In section 3 the experimental p LDOS of graphite obtained from the K x-ray absorption spectra and the K IXS spectra are compared with the theoretical spectra calculated by the full multiple-scattering method.

2. General theory for the core-level contributions to the IXS spectra

To calculate the IXS amplitudes within the one-electron approximation we have included the first- and the second-order processes described by the diagrams shown in figure 1. Figure 1(a) shows the first-order contribution resulting from the term $\hat{W}_{e\gamma}^{(2)}$ in (1). Figures 1(b)–1(e) give all the second-order contributions resulting from the term $\hat{W}_{e\gamma}^{(1)}$. From these diagrams the following expression for the IXS amplitude T can be derived:

$$T = \frac{2\pi e^2\hbar}{mcV(k_0k_1)^{1/2}}\left((e_0\cdot e_1)\langle\varphi_i|\exp(\mathrm{i}q\cdot\hat{r})|\varphi_0\rangle + \frac{1}{m}\sum_j \frac{\langle\varphi_i|\exp(-\mathrm{i}k_1\cdot\hat{r})(e_1\cdot\hat{p})|\varphi_j\rangle\langle\varphi_j|\exp(\mathrm{i}k_0\cdot\hat{r})(e_0\cdot\hat{p})|\varphi_0\rangle}{\hbar\omega_0+\varepsilon_0-\varepsilon_j+\mathrm{i}\eta} + \frac{1}{m}\sum_j \frac{\langle\varphi_i|\exp(\mathrm{i}k_0\cdot\hat{r})(e_0\cdot\hat{p})|\varphi_j\rangle\langle\varphi_j|\exp(-\mathrm{i}k_1\cdot\hat{r})(e_1\cdot\hat{p})|\varphi_0\rangle}{-\hbar\omega_1-\varepsilon_0-\varepsilon_j+\mathrm{i}\eta}\right) \tag{2}$$

where k_0, ω_0, e_0 and k_1, ω_1, e_1 are the wavevectors, frequencies and polarization vectors of the linearly polarized photons for the initial and final states, respectively, of the process; $|\varphi_0\rangle$, ε_0, $|\varphi_j\rangle$, ε_j and $|\varphi_i\rangle$, ε_i are the initial, intermediate and final wavefunctions and energies, respectively, of the excited electron; V is the normalization volume for the photon states; $q = k_0 - k_1$ is the transferred momentum.

It is worth noting that the summation in the second and the third terms in (2) is taken over both unoccupied and occupied intermediate one-electron states j. To show this, one should take into account that the second term in (2) results from figures 1(b) and 1(d) and the third term results from figures 1(c) and 1(e).

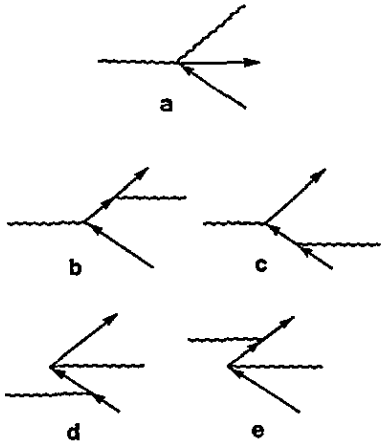

Figure 1. Diagrams which describe the first- and second-order contributions to the IXS amplitude.

To overcome the difficulties which arise owing to the summation in (2) over numerous intermediate states j, it is useful to introduce the one-electron Green function (GF) $\hat{G}_\varepsilon^+$ [4]:

$$\hat{G}_\varepsilon^+ = \sum_j \frac{|\varphi_j\rangle\langle\varphi_j|}{\varepsilon - \varepsilon_j + \mathrm{i}\eta}.$$

Substituting this expression in (2), one represents the second and the third terms in the large parentheses as follows:

$$\frac{1}{m}\int \varphi_i^*(r)\exp(-\mathrm{i}k_1\cdot r)(e_1\cdot\hat{\rho})G_E^+(r,r')\exp(\mathrm{i}k_0\cdot r')(e_0\cdot\hat{\rho})\varphi_0(r')\,\mathrm{d}^3r\,\mathrm{d}^3r' + \frac{1}{m}\int \varphi_i^*(r)\exp(\mathrm{i}k_0\cdot r)(e_0\cdot\hat{\rho})G_{-E'}^+(r,r')\exp(-\mathrm{i}k_1\cdot r')(e_1\cdot\hat{\rho})\varphi_0(r')\,\mathrm{d}^3r\,\mathrm{d}^3r' \tag{3}$$

where $E = \hbar\omega_0 + \varepsilon_0$, $E' = \hbar\omega_1 - \varepsilon_0$.

Since we treat hereafter only K-excitation processes, the radius r_0 of the atomic orbital $\varphi_0(r)$ is small. Let the x-rays considered satisfy the condition $k_0 r_0 \ll 1$ ($\hbar\omega_0 \ll 25$ keV for carbon atoms). In this case the dipole approximation may be used in the first-order matrix element in equation (2):

$$\langle\varphi_i|\exp(\mathrm{i}q\cdot r)|\varphi_0\rangle \simeq \langle\varphi_i|\mathrm{i}q\cdot r|\varphi_0\rangle.$$

The GF $G_{-E'}^+(r,r')$ rapidly decreases with increasing $|r-r'|$ owing to the large negative value of the GF energy parameter $-E'$. This enables us to use the dipole approximation also in the second term in (3). Within this approximation, one has $\exp(\mathrm{i}k_0\cdot r) \simeq \exp(\mathrm{i}k_1\cdot r') \simeq 1$.

The GF $G_E^+(r,r')$ does not decrease with increasing $|r-r'|$ but it oscillates rapidly. Taking this into account, one can show that the main contribution to the integral over r in the first term in (3) is provided by a small region near the centre of the excited atom. Consequently the dipole approximation may be used to calculate this term too. As a result we have

$$T \simeq \frac{2\pi e^2\hbar}{mcV(k_0k_1)^{1/2}}\left(\langle\varphi_i|\mathrm{i}q\cdot r(e_0\cdot e_1)\varphi_0\rangle + \langle\varphi_i|\frac{1}{m}(e_1\cdot\hat{\rho})G_E^+(e_0\cdot\hat{\rho})|\varphi_0\rangle\right.$$

$$+ \langle\varphi_i|\frac{1}{m}(e_0\cdot\hat{\rho})G^+_{-E'}(e_1\cdot\hat{\rho})|\varphi_0\rangle\Big)$$

$$= \frac{2\pi e^2\hbar}{mcV(k_0k_1)^{1/2}}(\varphi_i \mid \Phi) \tag{4}$$

where

$$\Phi(r) = \Phi_1(r) + \Phi_2(r) \qquad \Phi_1(r) = \mathrm{i}q\cdot r(e\cdot r(e_0\cdot e_1)\varphi_0(r)$$

$$\Phi_2(r) = \frac{1}{m}(e_1\cdot\hat{\rho})\int G^+_E(r,r')(e_0\cdot\hat{\rho})\varphi_0(r')\,\mathrm{d}^3r' \tag{5}$$

$$+\frac{1}{m}(e_0\cdot\hat{\rho})\int G^+_{-E'}(r,r')(e_1\cdot\hat{\rho})\varphi_0(r')\,\mathrm{d}^3r'.$$

Using the Fermi golden rule, one easily arrives at the following expression for the double-differential IXS cross section per one K-shell electron:

$$\frac{\mathrm{d}^2\sigma}{\mathrm{d}\Omega\,\mathrm{d}(\hbar\omega_1)} = r_0^2\frac{\omega_1}{\omega_0}M \tag{6}$$

where r_0 is the classical electron radius,

$$M = \sum_i |\langle\varphi_i|\Phi\rangle|^2\delta(\hbar\omega_0 + \varepsilon_0 - \hbar\omega_1 - \varepsilon_i). \tag{7}$$

Taking into account the properties of the function $\Phi(r)$, which is defined in (5), one concludes that the main contribution to the matrix element $\int\varphi_i^*(r)\Phi(r)\,\mathrm{d}^3r$ is provided by a small region near the centre of the excited atom. As was shown many years ago in the XAS theory [4, 5], expressions such as (7) may be simplified by the following transformation:

$$M = -\frac{1}{\pi}\int\Phi^*(r)\,\mathrm{Im}[G^+_\varepsilon(r,r')]\Phi(r')\,\mathrm{d}^3r\,\mathrm{d}^3r' \tag{8}$$

where the GF energy parameter $\varepsilon = \hbar\omega_0 + \varepsilon_0 - \hbar\omega_1$ is determined by the energy conservation law. Since we treat here only near-edge excitation processes, this parameter should be close to the conduction band bottom of the crystal. In the case of graphite we shall consider ε to be within the π^* and σ^* bands.

To calculate the integral (8), one needs to know the GF $G^+_\varepsilon(r,r')$ near the centre of the excited atom where the crystalline potential is spherical with respect to the atomic centre. Since the imaginary part of the GF obeys the homogeneous Schrödinger equation for both r and r' arguments, the following expansion for $-(1/\pi)\,\mathrm{Im}[G^+_\varepsilon(r,r')]$ takes place near the atomic centre:

$$-\frac{1}{\pi}\,\mathrm{Im}[G^+_\varepsilon(r,r')] = \sum_{L,L'}F_{LL'}R_{\varepsilon l}(r)Y_L(\hat{r})R_{\varepsilon l'}(r')Y_{L'}(\hat{r}') \tag{9}$$

where $R_{\varepsilon l}(r)$ is the real regular solution of the radial Schrödinger equation for the orbital momentum l and the energy ε; $Y_L(\hat{r})$ are the real spherical harmonics, where $L \equiv (l,m)$, $\hat{r} = r/r$ and $F_{LL'}$ are real coefficients which can be either calculated or determined from the experimental data. Of course, before determining these coefficients, the function $R_{\varepsilon l}(r)$ should be normalized.

To ascertain the physical meaning of the coefficients $F_{LL'}$, we take into account that

$$-\frac{1}{\pi}\int_{r<R_0}\mathrm{Im}[G_\varepsilon^+(r,r)]\,\mathrm{d}^3r=\sum_i\int_{r<R_0}|\varphi_i(r)|^2\delta(\varepsilon-\varepsilon_i)\,\mathrm{d}^3r=N_\varepsilon(R_0)$$

is the number of electron states per unit energy inside a sphere of radius R_0. Employing (8), one arrives at a useful formula for $N_\varepsilon(R_0)$:

$$N_\varepsilon(R_0)=\sum_L F_{LL}\int_0^{R_0}R_{\varepsilon l}^2(r)r^2\,\mathrm{d}r \tag{10}$$

where the radius R_0 should be so small that the expansion (8) was valid for $r\leqslant R_0$.

According to (10), the expression $F_{LL}\int_0^{R_0}R_{\varepsilon l}^2(r)r^2\,\mathrm{d}r$ may be considered to be the number of partial L states per unit energy inside the sphere of radius R_0 around the atomic centre (partial LDOS). Since we study low-Z atom K excitation into the electron states which are close to the conduction band bottom, only the terms with $l=0$ and $l=1$ may be involved in (8). Taking into account the symmetry of the graphite crystal and taking the x_3 axis of the coordinate system perpendicular to the basal planes of graphite, we have:

$$\begin{aligned}-\frac{1}{\pi}\mathrm{Im}[G_\varepsilon^+(r,r')]&=F_sR_{\varepsilon0}(r)Y_{00}(\hat r)R_{\varepsilon0}(r')Y_{00}(\hat r')+F_\pi R_{\varepsilon1}(r)Y_{13}(\hat r)R_{\varepsilon1}(r')Y_{13}(\hat r')\\&\quad+F_\sigma R_{\varepsilon1}(r)R_{\varepsilon1}(r')[Y_{11}(\hat r)Y_{11}(\hat r')+Y_{12}(\hat r)Y_{12}(\hat r')]\end{aligned} \tag{11}$$

where

$$F_s=F_{00,00}\qquad F_\pi=F_{13,13}\qquad F_\sigma=F_{11,11}=F_{12,12}$$

$$Y_{1m}=\left(\frac{3}{4\pi}\right)^{1/2}\frac{r_m}{r}.$$

Before substituting the expansion (11) into (8), one should study the symmetry of the functions $\Phi_1(r)$ and $\Phi_2(r)$ defined in (5). Since $\varphi_0(r)$ is the s-symmetry function, $\Phi_1(r)$ is obviously the superposition of p-symmetry functions. To clarify the symmetry of the function $\Phi_2(r)$, one should first take into account in (5) that, owing to the large values of the energy parameters E and $-E'$ of the GFs $G_E^+(r,r')$ and $G_{-E'}^+(r,r')$, the effect of neighbouring atoms on these functions is negligible and hence they can be calculated for the spherical potential of the excited atom. As a result, the integrals $\int G_E^+(r,r')\hat\rho_n\varphi_0(r')\,\mathrm{d}^3r'$ and $\int G_{-E'}^+(r,r')\hat\rho_n\varphi_0(r')\,\mathrm{d}^3r'$ in (5) (where $\hat\rho_n=-i\hbar\partial/\partial r_n'$) are the p-symmetry functions and consequently the function $\Phi_2(r)$ is the superposition of s and d terms.

Putting the expansion (11) in (8) and taking into account the symmetry of the functions $\Phi_1(r)$ and $\Phi_2(r)$, after simple calculations one obtains

$$M=(e_0\cdot e_1)\{[F_\pi q_3^2+F_\sigma(q_1^2+q_2^2)]K_1^2+F_s|K_0|^2\} \tag{12}$$

where

$$\frac{1}{m}\int R_{\varepsilon0}(r)\hat\rho_t\left(\int G_E^+(r,r')\hat\rho_n\varphi_0(r')\,\mathrm{d}^3r'+\int G_{-E'}^+(r,r')\hat\rho_n\varphi_0(r')\,\mathrm{d}^3r'\right)\mathrm{d}^3r=K_0\delta_{tn} \tag{13}$$

and

$$(\tfrac{1}{3})^{1/2}\int R_{\varepsilon1}(r)r\varphi_0(r)r^2\,\mathrm{d}r=K_1. \tag{14}$$

The expression for the double-differential cross section now takes the final form

$$\frac{d^2\sigma}{d\Omega\, d(\hbar\omega_1)} = r_0^2 \frac{\omega_1}{\omega_0}(e_0 \cdot e_1)^2 S(q, \omega_0) \tag{15}$$

where

$$S(q, \omega_0) = (F_\pi q_\parallel^2 + F_\sigma q_\perp^2)K_1^2 + F_s|K_0|^2$$

is the dynamic structure factor which has been determined in [2] for the graphite crystal by the experimental IXS spectra, $q_\parallel = q_3$ is the projection of the vector q on the x_3 axis, and $q_\perp$ is its projection on the basal planes of graphite.

Since the coefficients K_0 and K_1 can be accurately determined by simple atomic calculations and the experimental IXS spectra can be measured for different directions and absolute values of the transferred momentum q, one is able, in principle, to determine F_s, F_σ and F_π from the experimental spectra. Of course, before calculating the coefficients K_0 and K_1, one should choose the norms of the wavefunctions $R_{\varepsilon 0}(r)$ and $R_{\varepsilon 1}(r)$. Let us normalize them as follows:

$$\begin{aligned} \int_0^{R_0} R_{\varepsilon 0}^2(r) r^2\, dr &= \int_0^{R_0} \varphi_{2s}^2(r) r^2\, dr \\ \int_0^{R_0} R_{\varepsilon 1}^2(r) r^2\, dr &= \int_0^{R_0} \varphi_{2p}^2(r) r^2\, dr \end{aligned} \tag{16}$$

where $\varphi_{2s}(r)$ and $\varphi_{2p}(r)$ are the 2s and 2p atomic radial wavefunctions of the free carbon atom.

Employing such normalization for the functions $R_{\varepsilon 0}(r)$ and $R_{\varepsilon 1}(r)$, one could interpret the coefficients F_s, F_π and F_σ in (12) and (15) in terms of the LCAO model. Within the framework of this model, one may consider that F_s is the number of 2s electron states per unit energy (2s LDOS), F_π is the number of π^*-type 2p states per unit energy ($2p_\pi^*$ LDOS), and $2F_\sigma$ is the number of σ^*-type 2p states per unit energy ($2p_\sigma^*$ LDOS). Naturally, such interpretation is possible only when ε is within π^* and σ^* bands. One should note that the defect of this interpretation is the dependence of the 2s and 2p LDOS on the parameter R_0. Fortunately, this dependence is not strong for comparatively small R_0 owing to the well known phenomenon of radial wavefunction shape conservation (i.e. the shapes of the $R_{\varepsilon 0}(r)$ and $R_{\varepsilon 1}(r)$ radial wavefunctions change slowly within a wide energy region for $r < R_1$, where R_1 is the position of the main maximum of the function $\varphi_{nl}(r)$).

Equation (13) is not suitable for calculating the coefficient K_0 because one needs to integrate in (13) the expression which contains the rapidly oscillating function $G_E^+(r, r')$. The calculations can be simplified if the following transformation of the matrix elements in (13) is carried out (see appendix):

$$\begin{aligned} K_0\delta_{in} = {} & \frac{E - \varepsilon_0}{E - \varepsilon_i} \int R_{\varepsilon 0}(r) \frac{\partial U(r)}{\partial r_i}\, d^3r \int G_E^+(r, r') r_n' \varphi_0(r')\, d^3r' \\ & + \frac{i}{\hbar} \frac{\varepsilon_i - \varepsilon_0}{E - \varepsilon_i} \int R_{\varepsilon 0}(r) \hat{p}_i r_n \varphi_0(r)\, d^3r \\ & + \frac{E' + \varepsilon_0}{E' + \varepsilon_i} \int R_{\varepsilon 0}(r) \frac{\partial U(r)}{\partial r_i}\, d^3r \int G_{-E'}^+(r, r') r_n' \varphi_0(r')\, d^3r' \\ & - \frac{i}{\hbar} \frac{\varepsilon_i - \varepsilon_0}{E' + \varepsilon_i} \int R_{\varepsilon 0}(r) \hat{p}_i r_n \varphi_0(r)\, d^3r \end{aligned} \tag{17}$$

where $U(r)$ is the atomic potential.

One can easily see that the main contributions in all terms in (17) are provided by the small region near the centre of the excited atom. As mentioned above, in this region the GFs $G_E^+(r, r')$ and $G_{-E'}^+(r, r')$ can be calculated for the spherical atomic potential. Using traditional one-centre expansion for the GF in (17) and integrating over angular arguments, one obtains

$$K_0 = \frac{1}{3}\left(\frac{E-\varepsilon_0}{E-\varepsilon_i}\int R_{\varepsilon 0}(r)\frac{\partial U(r)}{\partial r}H_{E1}^+(r_>)R_{E1}(r_<)r'\varphi_0(r')r^2\,\mathrm{d}r r'^2\,\mathrm{d}r'\right.$$
$$+\frac{\mathrm{i}}{\hbar}\frac{\varepsilon_i-\varepsilon_0}{E-\varepsilon_i}\int R_{\varepsilon 0}(r)r\frac{\partial\varphi_0}{\partial r}r^2\,\mathrm{d}r$$
$$+\frac{E'+\varepsilon_0}{E'+\varepsilon_i}\int R_{\varepsilon 0}(r)\frac{\partial U(r)}{\partial r}H_{(-E')1}^+(r_>)R_{(-E')1}(r_<)r'\varphi_0(r')r^2\,\mathrm{d}r r'^2\,\mathrm{d}r'$$
$$\left.-\frac{\mathrm{i}}{\hbar}\frac{\varepsilon_i-\varepsilon_0}{E'+\varepsilon_i}\int R_{\varepsilon 0}(r)r\frac{\partial\varphi_0}{\partial r}r^2\,\mathrm{d}r\right) \tag{18}$$

where the functions H_{El}^+ and R_{El} are the solutions of the atomic radial Schrödinger equation which satisfy the same boundary conditions as the functions h_{El}^+ and j_{El}.

We have calculated the coefficients $|K_0|^2$ and K_1^2 through equations (14) and (18) using a self-consistent potential of the free carbon atom. Normalization of the functions $R_{\varepsilon 1}(r)$ and $R_{\varepsilon 0}(r)$ have been carried out according to (16) for $R_0 = 1.34$ au (one half of the interatomic distance between the nearest carbon atoms in the graphite basal plane). The results obtained for the initial photon energy $\hbar\omega_0 = 8$ keV are presented in figure 2 where the coefficients $|K_0|^2$ (curve 1) and K_1^2 (curve 2) versus the photon energy loss are shown. We see that owing to the above-mentioned phenomenon of radial wavefunction shape conservation the coefficients $|K_0|^2$ and K_1^2 do not depend strongly on the photon energy loss. For qualitative processing, the experimental spectra that we have employed average magnitudes for π^* and σ^* bonds of these coefficients. The dependence of the average magnitudes of the coefficients $|K_0|^2$ (curve 1) and K_1^2 (curve 2) on the initial photon energy $\hbar\omega_0$ is demonstrated in figure 3. The results obtained show that for large photon energies ($\hbar\omega_0 \gg 2$ keV) the second-order contribution to the total IXS cross section, which is proportional to $|K_0|^2 F_s$, is small and should be taken into account only in the case of x-ray forward scattering. On the contrary, for $\hbar\omega_0 < 2$ keV the second-order contribution is sufficiently large and hence, using soft x-rays, one can study the 2s LDOS in the crystals by the IXS spectra above the K edge. It is worth noting that the mean free paths of 2 keV x-rays in the crystals, which contain low-Z atoms, are not too small.

We would like to emphasize that the information about the 2s LDOS cannot be obtained by the usual XAS method for low-Z elements owing to the dipole selection rules but it is interesting. For instance, when this information is obtained for diamond, it enables one to solve the well known problem [6] of the deep s excitation level which is expected to appear in the forbidden gap owing to the K-hole potential influence. It is easy to show that in the case of diamond the expression for the double-differential IXS cross section takes the form

$$\frac{\mathrm{d}\sigma}{\mathrm{d}\Omega\,\mathrm{d}(\hbar\omega_1)} = r_0^2\frac{\omega_1}{\omega_0}(e_0\cdot e_1)^2 S(q,\omega_0)$$
$$S(q,\omega_0) = F_s|K_0|^2 + F_\sigma q^2 K_1^2 \tag{19}$$

where $3F_\sigma$ is the 2p LDOS, and the other notation is the same as in (15).

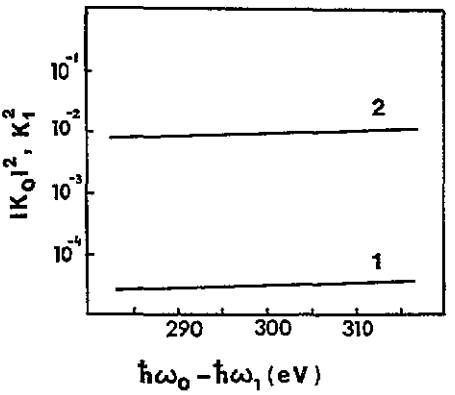

Figure 2. The coefficients $|K_0|^2$ (line 1) and K_1^2 (line 2) versus the photon energy loss for the initial photon energy $\hbar\omega_0 = 8$ keV.

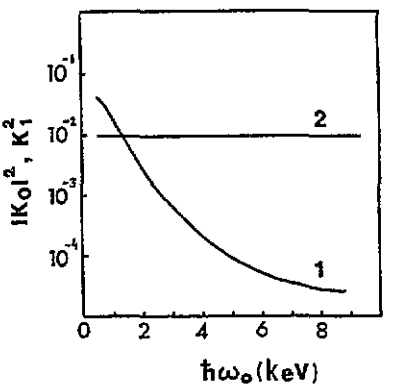

Figure 3. Averaged magnitudes of the coefficients $|K_0|^2$ (line 1) and K_1^2 (line 2) versus the initial photon energy.

3. Comparison of the experimental and theoretical π^* and σ^* LDOSs for graphite

To obtain the experimental π^* and σ^* LDOSs for graphite we employed the IXS spectra presented in [2] and the C x-ray absorption spectra presented in [7]. In [2] the absolute values of the IXS cross sections have been measured for the initial photon energy $\hbar\omega_0 = 8$ keV. In this case the contribution of the second-order terms to the cross section as has been shown in section 2 is negligible and hence

$$S(q, \omega_0) = (F_\pi q_\parallel^2 + F_\sigma q_\perp^2) K_1^2$$

(see equation (15)). Using this equation and average magnitudes of the coefficient K_1^2 for π^* and σ^* bands we have calculated the π^* and σ^* LDOSs (F_π and $2F_\sigma$) using the experimental IXS spectra. The results obtained are shown in figure 4 (dotted curves). One may obtain information about the LDOS by also employing absolute values of the x-ray absorption cross sections. The K-shell contribution σ_K to this cross section in the case of the graphite crystal takes the form

$$\sigma_K = 8\pi^2 \alpha \hbar\omega_0 (\cos^2\theta F_\sigma + \sin^2\theta F_\pi) K_1^2 \tag{20}$$

where θ is the angle between the x-ray polarization vector e and the basal planes of graphite.

Unfortunately the C K x-ray absorption spectra for the graphite crystal presented in [7] have not been measured in the absolute scale. In [7] the C K x-ray absorption spectra were measured for $\pi/3 \geqslant \theta \geqslant 0$ where θ is the angle between the basal planes in graphite and the x-ray polarization vector. For $\theta = 0$ they obtained the spectrum associated with the electron transition into σ^* states. To obtain the pure contribution of π^* electron states we have carried out a decomposition of the spectrum measured for $\theta = \pi/3$. As a result we have obtained the cross sections in arbitrary units which are proportional to

$$\sigma_K^{(\sigma)} = 8\pi^2 \alpha \hbar\omega_0 F_\sigma K_1^2$$

and

$$\sigma_K^{(\pi)} = 8\pi^2 \alpha \hbar\omega_0 F_\pi K_1^2$$

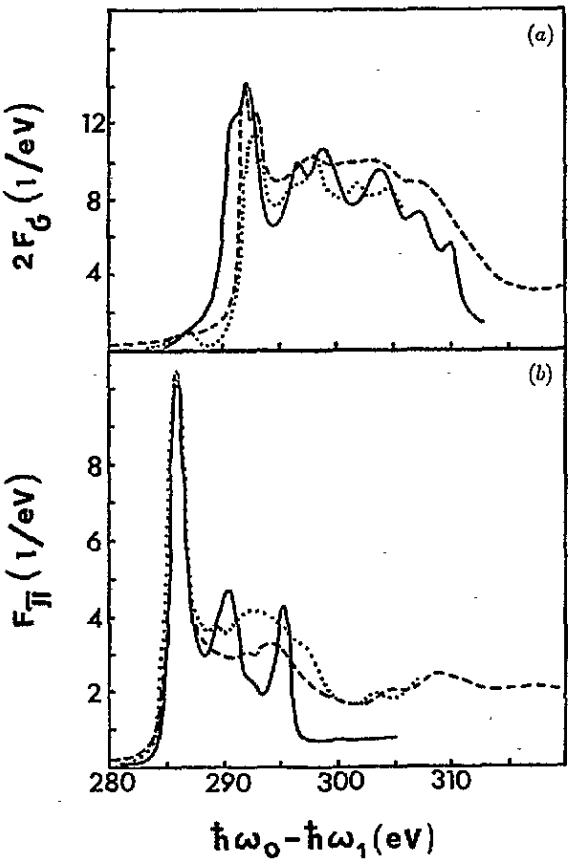

Figure 4. (*a*) σ^* LDOS and (*b*) π^* LDOS in electron number per electronvolt versus the photon energy loss (IXS spectra) or the photon energy (XAS): ——, results of the full multiple-scattering calculations; ·····, results obtained from the IXS spectra [2], ----, results obtained from XAS [7].

(see equation (20)). To calculate the absorption cross sections we have used the absolute value of the carbon atom scattering factor f presented in the tables in [8] for the photon energy $\hbar\omega_0 = 340$ eV which exceeds the absorption edge by more than 40 eV. In this region the absorption cross section oscillations are of EXAFS character and hence the atomic cross section for the graphite crystal almost coincides with that for the isolated carbon atom, $4\pi(e^2/mc\omega)\,\mathrm{Im}(f)$. Since the C K x-ray absorption spectra have been measured in [7] up to this energy, we are able to use the magnitude $\mathrm{Im}(f)$ from [8] for the normalization of the experimental absorption spectra. After simple calculations we have obtained π^* and σ^* LDOSs which are also presented in figure 4 (dashed curves). It is worth noting that the π^* and σ^* LDOSs obtained from the experimental C K x-ray absorption and IXS spectra appear to be quite close to each other. It is interesting to determine from the LDOS obtained the number of C 2p states per π^* band and σ^* band. To do this we have calculated the integrals

$$N_{2p}^{\pi^*} = \int_{\omega_1^\pi}^{\omega_2^\pi} F_\pi \,\mathrm{d}\omega$$
$$N_{2p}^{\sigma^*} = \int_{\omega_1^\sigma}^{\omega_2^\sigma} 2F_\sigma \,\mathrm{d}\omega \qquad (21)$$

where ω is the photon energy in the case of K x-ray absorption spectra and the photon energy loss in the case of IXS spectra; $\omega_1^\pi = 20.66$ Ryd, $\omega_2^\pi = 22.25$ Ryd, $\omega_1^\sigma = 20.66$ Ryd and $\omega_2^\sigma = 23.43$ Ryd. The results obtained are presented in table 1.

Table 1. The calculated and experimental numbers of 2p electron states per σ^* and π^* bands for graphite.

	Calculated numbers		Experimental numbers	
	ground state	1s-hole state	IXS spectra	XAS
$N_{2p}^{\sigma^*}$	2.57	1.98	2.02	2.24
$N_{2p}^{\pi^*}$	1.12	0.51	0.67	0.56

The calculations of π^* and σ^* LDOSs for graphite have been carried out by the traditional full multiple-scattering method using GF formalism and the muffin-tin (MT) approximation for the crystalline potential. It is worth noting that the MT approximation for the potential of the layered crystal is not quite satisfactory. Indeed, the interatomic potential averaged along the electron paths joining atoms of one layer is essentially more attractive than that averaged along the paths joining atoms of different layers. Since σ^* wavefunctions in graphite are localized mainly near the layer which contains the absorbing atom and π^* wavefunctions deeply penetrate into the interlayer space, one deduces that the interstitial potential (MT zero) used for the π^* LDOS calculations should be less attractive than that used for the σ^* LDOS calculations. Estimation of the interstitial potential shift is complicated and we consider these potentials to be the adjustable parameters.

We have considered the potential inside the carbon atomic spheres to be equal to the free-atom potential calculated by the Herman–Scillman [9] algorithm. To include the K-hole presence and the extra-atomic relaxation we have calculated the potential of the ionized carbon atom for the configuration $1s^1 2s^2 2p^3$. For the empty electron states the Diroc–Hare [10] exchange potential has been employed. The interstitial potential for the σ^* calculations has been chosen in such a way that the potential discontinuity at the atomic sphere surface was as small as possible to ensure that the σ^* LDOS is sufficiently contrasting. The interstitial potential for the π^* calculations has been chosen to provide the energy difference between σ^* and π^* bands in agreement with experiment.

The scattering phase shift δ_l for the carbon atomic spheres has been considered to be equal to zero for $l \geqslant 2$. To calculate the σ^* LDOS the plane 73-atom cluster has been used. To calculate the π^* LDOS we have used a five-layered cluster which contains 89 atoms. The theoretical LDOSs obtained in this way which are presented in figure 4 (solid curves) appear to be in reasonable agreement with the experimental LDOSs. This result confirms the adequacy of the one-electron theoretical model and the method of experimental spectra processing proposed above.

Using equation (21) we have calculated the theoretical magnitudes of the numbers $N_{2\rho}^{\sigma^*}$ and $N_{2\rho}^{\pi^*}$ of C 2p states per σ^* band and π^* band which are presented in table 1. We see that these numbers are in good agreement with those calculated from the experimental x-ray absorption and IXS spectra. In table 1 the thoeretical numbers $N_{2\rho}^{\sigma^*}$ and $N_{2\rho}^{\pi^*}$ calculated for the ground state of the graphite crystal are also presented. Comparison of the results obtained shows that the effect of the K-hole potential on the $N_{2\rho}^{\pi^*}$ is more substantial than on $N_{2\rho}^{\sigma^*}$. The large magnitudes of the numbers $N_{2\rho}^{\sigma^*}$ and $N_{2\rho}^{\pi^*}$ for the ground state of the crystal in comparison with those which are predicted by the simple tight-bonding model can be explained by the overlapping of the neighbouring-atom 2p and 2s wavefunctions.

Acknowledgments

This work was supported, in part, by a Soros Foundation Grant awarded by the American Physical Society and by grant 15-51-14 at 1992 awarded by the Ministry of Science, Higher Education and Technological Policy of the Russian Federation.

Appendix

To obtain equation (17) we have started from equation (4). To simplify the calculations of the matrix elements

$$\langle\varphi_i|(e_1\cdot\hat{\rho})\hat{G}_E^+(e_0\cdot\hat{\rho})|\varphi_0\rangle=\sum_{t,n}e_{1t}e_{0n}\langle\varphi_i|\hat{\rho}_t\hat{G}_E^+\hat{\rho}_n|\varphi_0\rangle$$

and

$$\langle\varphi_i|(\hat{e}_0\cdot\hat{\rho})\hat{G}_{-E'}^+(\hat{e}_1\cdot\hat{\rho})|\varphi_0\rangle=\sum_{t,n}e_{0t}e_{1n}\langle\varphi_i|\hat{\rho}_t\hat{G}_{-E'}^+\hat{\rho}_n|\varphi_0\rangle$$

the following transformations have been carried out:

$$\langle\varphi_i|[\hat{H},\hat{\rho}_t]\hat{G}_E^+\hat{\rho}_n|\varphi_0\rangle=\langle\varphi_i|\hat{\rho}_t\hat{\rho}_n|\varphi_0\rangle-(E-\varepsilon_i)\langle\varphi_t|\hat{\rho}_t\hat{G}_E^+\hat{\rho}_n|\varphi_0\rangle.$$

Consequently

$$\langle\varphi_i|\hat{\rho}_t\hat{G}_E^+\hat{\rho}_n|\varphi_0\rangle=\frac{1}{E-\varepsilon_i}\left(\langle\varphi_i|\hat{\rho}_t\hat{\rho}_n|\varphi_0\rangle-\mathrm{i}\hbar\langle\varphi_i|\frac{\partial U}{\partial r_t}\hat{G}_E^+\hat{\rho}_n|\varphi_0\rangle\right).$$

Then,

$$\langle\varphi_i|\frac{\partial U}{\partial r_t}\hat{G}_E^+[\hat{r}_n,\hat{H}]|\varphi_0\rangle=\langle\varphi_i|\frac{\partial U}{\partial r_t}\hat{r}_n|\varphi_0\rangle-(E-\varepsilon_0)\langle\varphi_i|\frac{\partial U}{\partial r_t}\hat{G}_E^+\hat{r}_n|\varphi_0\rangle$$

$$\mathrm{i}\hbar\langle\varphi_i|\frac{\partial U}{\partial r_t}\hat{G}_E^+\hat{\rho}_n|\varphi_0\rangle=m\left(\langle\varphi_i|\frac{\partial U\hat{r}_n}{\partial r_t}|\varphi_0\rangle-(E-\varepsilon_0)\langle\varphi_i|\frac{\partial U}{\partial r_t}\hat{G}_E^+\hat{r}_n|\varphi_0\rangle\right).$$

As a result we arrive at the equation

$$\langle\varphi_i|\hat{\rho}_t\hat{G}_E^+\hat{\rho}_n|\varphi_0\rangle=m\frac{E-\varepsilon_0}{E-\varepsilon_i}\langle\varphi_i|\frac{\partial U}{\partial r_t}\hat{G}_E^+\hat{r}_n|\varphi_0\rangle+\frac{m}{\mathrm{i}\hbar}\frac{\varepsilon_0-\varepsilon_i}{E-\varepsilon_i}\langle\varphi_i|\hat{r}_n\hat{\rho}_t|\varphi_0\rangle. \tag{A1}$$

Conducting similar transformations of the term which contains the GF $\hat{G}_{-E'}^+$ we have

$$\langle\varphi_i|\hat{\rho}_t\hat{G}_{-E'}^+\hat{\rho}_n|\varphi_0\rangle=m\frac{E'+\varepsilon_0}{E'+\varepsilon_i}\langle\varphi_i|\frac{\partial U}{\partial r_t}\hat{G}_{-E'}^+\hat{r}_n|\varphi_0\rangle+\frac{m}{\mathrm{i}\hbar}\frac{\varepsilon_0-\varepsilon_i}{-E'-\varepsilon_i}\langle\varphi_i|\hat{r}_n\hat{\rho}_t|\varphi_0\rangle. \tag{A2}$$

Substituting (A1) and (A2) in (4), one obtains

$$\begin{aligned}T=\frac{2\pi\hbar e^2}{mcV(k_0k_1)^{1/2}}\Bigg[&\langle\varphi_i|\mathrm{i}\boldsymbol{q}\cdot\boldsymbol{r}(e_0\cdot e_1)|\varphi_0\rangle\\&+\sum_{t,n}e_{1t}e_{0n}\left(\frac{E-\varepsilon_0}{E-\varepsilon_i}\langle\varphi_i|\frac{\partial U}{\partial r_t}\hat{G}_E^+\hat{r}_n|\varphi_0\rangle+\frac{\mathrm{i}}{\hbar}\frac{\varepsilon_i-\varepsilon_0}{E-\varepsilon_i}\langle\varphi_i|\hat{r}_n\hat{\rho}_t|\varphi_0\rangle\right)\\&+\sum_{t,n}e_{0t}e_{1n}\left(\frac{E'+\varepsilon_0}{E'+\varepsilon_i}\langle\varphi_i|\frac{\partial U}{\partial r_t}\hat{G}_{-E'}^+\hat{r}_n|\varphi_0\rangle-\frac{\mathrm{i}}{\hbar}\frac{\varepsilon_i-\varepsilon_0}{E'+\varepsilon_i}\langle\varphi_i|\hat{r}_n\hat{\rho}_t|\varphi_0\rangle\right)\Bigg].\end{aligned} \tag{A3}$$

Using equation (A3) and carrying out transformations similar to those which have resulted in equation (12), one arrives at equation (17).

References

[1] Schulke W, Berthold A and Kaprolat A 1988 *Phys. Rev. Lett.* **60** 2217
[2] Schulke W, Bonse U, Nagasawa H, Kaprolat A and Berthold A 1988 *Phys. Rev.* B **38** 2112
[3] Nozieres P and Pines D 1959 *Phys. Rev.* **113** 1254
[4] Ashley C A and Doniach S 1975 *Phys. Rev.* B **11** 1279
[5] Vedrinskii R V and Novakovich A A 1975 *Fiz. Metal. Metalloved.* **39** 7
[6] Jackson K A and Pederson M R 1991 *Phys. Rev. Lett.* **67** 2521
[7] Blocker J, Werner H, Herein D, Schlogl R, Schedel-Niedrig Th, Keil M and Bradshaw A 1992 *Mater. Sci. Forum* **91–93** 337
[8] Henke B L, Lee P, Tanaka T J, Shimabukuro R L and Fujikawa B K 1982 *At. Data Nucl. Data Tables* **27** 1
[9] Herman F and Skillman S 1963 *Atomic Structure Calculation* (Englewood Cliffs, NJ: Prentice-Hall)
[10] Chou S-H, Rehr J J and Stern E A 1987 *Phys. Rev.* B **35** 2604